ALLOY DEVELOPMENT OF NICKEL-BASED SUPERALLOY WELD FILLER METALS USING COMPUTATIONAL THERMODYNAMICS

J. M. Vitek[1]
D. W. Gandy[2]
S. S. Babu[1]
G. J. Frederick[2]
[1]Oak Ridge National Laboratory
P. O. Box 2008
Oak Ridge, Tennessee 37831-6096
[2]EPRI
P. O. Box 217097
Charlotte, North Carolina 28262

ALLOY DEVELOPMENT OF NICKEL-BASED SUPERALLOY WELD FILLER METALS USING COMPUTATIONAL THERMODYNAMICS

J. M. Vitek[1]
D. W. Gandy[2]
S. S. Babu[1]
G. J. Frederick[2]
[1]Oak Ridge National Laboratory
P. O. Box 2008
Oak Ridge, Tennessee 37831-6096
[2]EPRI
P. O. Box 217097
Charlotte, North Carolina 28262

Abstract

Weld repairs of gamma-prime-strengthened nickel-based superalloys such as IN738, IN939, Rene80 and GTD111 typically use lower strength solid solution filler metals, thereby limiting the weld repair to low stress regions. The use of gamma-prime-strengthened filler metals is also limited because of issues related to weldability and as-welded properties. These problems are often related to the formation of deleterious phases during welding. This study was aimed at examining alloy modifications to gamma-prime-strengthened alloys that will avoid the formation of these undesirable phases and will yield improved filler metal alloys for welding. Computational thermodynamics was used in the study to examine the influence of alloy modifications on the phase stability of nickel-based superalloys. This approach can take into account many of the complex interactions among alloying additions, and it provides a simple and efficient means for alloy optimization. The results of the calculations are presented. The effect of alloying additions on the stability of carbides and undesirable phases such as eta phase, sigma phase, and P-phase is described. The results often show very complex interactions but they can be readily explained and understood. These calculations show the potential of using computational thermodynamics as a valuable tool in alloy design and optimization.

Introduction

The objective of this study was to improve weld filler metals that can be used to repair or refurbish turbine engine components made of nickel-based superalloys such as IN738, IN939, Rene80, and GTD111. Lower strength, solid solution filler metals, such as IN625, are commonly used in the industrial gas turbine industry to repair rotating turbine blades. While these alloys offer excellent weldability and ductility, they suffer considerably in overall high-temperature strength and performance. As a result, these fillers are used only to repair lower-stress regions of blade airfoils and other parts. The availability of high-strength precipitation-strengthened filler metals for weld repair of nickel-based superalloy parts is highly desirable to allow repairs to be performed over the entire component. Unfortunately, existing precipitation-strengthened alloys such as IN738, IN939, Rene80, and GTD111 are not readily weldable or they do not have optimal weld properties. Laser welding often leads to inferior weld properties as a result of the presence of deleterious phases. This study was aimed at identifying alloy compositions that would eliminate such phases and thereby improve weldability and/or properties.

Conventional alloy development is costly and time consuming because it involves several trial and error iterations of processing and evaluation. In addition, alloy optimization is very difficult to achieve because it is often impossible to control or evaluate all relevant variables. This entire process can be shortened with the use of computational thermodynamics, which provides a convenient means for assessing phase stability as a function of alloy composition and temperature. This approach was used extensively to examine the influence of alloying additions on phase stability in alloys comparable to IN738, IN939, Rene80 and GTD111 in an effort to obtain a filler metal composition that would be superior to those that are currently in use. The calculations indicated the limits for various additions, beyond which undesirable phases such as sigma phase, eta phase, mu phase, and P-phase were stable[1]. The calculations also provide valuable information with regard to the temperature ranges for processing. This paper will present some of the results of these calculations that provided guidance for alloy development and optimization.

Calculation Procedures

In the last decade, commercial packages have become available for the calculation of phase stability in multi-component systems. Several different packages are commercially available (1-5). The same general approach is utilized in all of these routines. The free energy of competing phases is modeled as a function of temperature, pressure and composition, and the software calculates the phases and their compositions that lead to the minimum free energy (i.e., equilibrium). Some flexibility exists in order to consider non-equilibrium behavior as well. The

---

[1] Sigma, eta, mu, and P phases are complex phases often associated with degradation in properties. Typical major constituents in each phase are: Cr, Co, Ni, Mo (sigma phase); Ni, Co, Cr, Ti (eta phase); Mo, W, Ni, Co, Cr (mu phase); and W, Mo, Cr, Ni, Co (P phase).

key to all of these computational tools is the database that contains all the relevant parameters to describe the functional behavior of the free energy. The unique feature of these computational thermodynamics tools is that multi-component systems corresponding to real commercial alloys, with ten or more components, can be readily modeled, and phase stability can be assessed with reasonable accuracy.

In the present work, the JMatPro software package (5) was utilized in conjunction with the Ni-DATA database (6). This 17-element database has been specifically developed for nickel-based superalloys and includes the following elemental additions to Ni: Al, B, C, Co, Cr, Fe, Hf, Mo, N, Nb, Re, Si, Ta, Ti, W, and Zr. Calculations were made over a wide temperature and composition range, with pressure fixed at one atmosphere. For the present calculations, potential dilution effects during welding were ignored.

Calculations for Base Alloys IN738, IN939, Rene80 and GTD111

As a reference, calculations were carried out for the four base materials, IN738, IN939, Rene80 and GTD111. Typical compositions for these alloys that were used in the calculations are given in Table 1. The results of the phase stability calculations are shown in Figure 1, as plots of wt % of various phases as a function of temperature. Starting at high temperatures, but below the solidus temperature, the equilibrium phase plots show a large solution temperature range with nearly 100% gamma and a small amount (1-2%) of MC carbide and very little (<0.1%) MB_2 boride. At lower temperatures, between 1120 and 1160°C, depending upon the specific alloy, gamma prime formation is predicted to begin. As the temperature drops below the gamma prime solvus, the amount of gamma prime phase continuously increases, eventually leveling off to values between 35 and 57 wt % gamma prime, depending upon the alloy. Additional phases are also predicted to form below the gamma prime solvus, and replacement of the high temperature MB_2 and MC phases by M_3B_2 and $M_{23}C_6$ is also found. Moreover, many potentially undesirable phases are predicted, including (a) eta phase formation in IN939 between 1050 and 1150°C, (b) sigma phase formation an all alloys below 850°C, (c) P-phase formation in Rene80 below ~900°C, and (d) mu phase formation in Rene80 below ~800°C.

Phase Stability Calculations for IN625 and Modified Alloys

Similar phase stability plots were calculated for IN625, which is a common filler metal used in welding the gamma prime strengthened alloys such as IN738, IN939, Rene80 and GTD111. The results are plotted in Figure 2. As noted earlier, this filler metal leads to a significant reduction in strength and the reasons behind this are clearly evident from the phase stability plots. Whereas IN738, IN939, Rene80 and GTD111 all have significant amounts (35 to 57 wt %) of gamma prime in a matrix of gamma phase, the IN625 has very little gamma prime (< 5%), and only at low temperatures. Instead, IN625 is hardened by a combination of solution hardening and limited precipitation hardening by Ni_3Nb (labeled “delta phase” in Figure 2). The calculations also show that sigma and mu phases are stable below ~900°C.

Additional calculations were made by varying the compositions of the gamma-prime-containing alloys in order to identify the effect of various changes in elemental concentrations. Unlike alloy development procedures that involve many iterations of casting and processing of new alloy compositions, computational thermodynamics allows one to easily and quickly investigate alloy modifications to determine trends and to identify potential improvements. Some of the observations and trends that were found will now be presented.

The predicted formation of eta phase in IN939 was studied in greater detail. The composition of the eta phase at 1120°C was found to be (wt %): Ni-2.16Al-17.1Co-0.29Cr-5.92Nb-2.14Ta-12.96Ti. The calculations for IN939 and for additional variations showed that eta typically formed when gamma prime formation was suppressed to lower temperatures and eta became unstable once gamma prime formation took place. Therefore, in spite of the fact that eta has an appreciable amount of Al and Ti, calculations were made for a modified composition in which Al was added in order to stabilize gamma prime and to prevent the transient formation of eta. This removed much of the eta phase, and a reduction of Nb led to the complete elimination of eta phase. These trends are shown in Figure 3, where the phase stability at 1120°C is plotted as a function of Al content (Figure 3a) and Nb content (Figure 3b). In these calculations, the composition in Table 1 for IN939 was used and only one element (either Al or Nb) was allowed to vary. Clearly, raising the Al content from the nominal value of 1.9 wt % leads to a reduction in eta phase while concurrently stabilizing gamma prime. A reduction in Nb from the nominal level of 1 wt % also leads to the destabilization of eta phase, but a simultaneous stabilization of gamma prime was not found.

The calculations for IN738, IN939, Rene80, and GTD111 show that at low temperatures (<900°C), some undesirable phases may become stable. Further calculations were made to understand in greater detail the effects of composition on the stability of the P and sigma phases. The P-phase composition in Rene80 at 800°C is (wt %) 31.37W-25.59Mo-18.49Ni-18.26Cr-6.29Ni and the sigma phase composition in IN939 at 800°C is (wt %) 58.02Cr-26.94Co-12.78Ni-2.26W. The calculations indicated that P-phase was very rich in Mo. Therefore, it was inferred that a reduction in Mo would help to remove the presence (as calculated) of P-phase. The effect of a change in Mo content, keeping all other additions constant at the values for Rene80 (see Table 1), is shown in Figure 4. The effect of Mo is clear; as assumed, increasing the Mo content increases the stability of P-phase. Such calculations can be used to identify the critical levels for various constituents. In the case of the Rene80 composition given in Table 1, Mo levels below 2.99 wt % will avoid P-phase formation.

With regard to the predicted sigma phase formation, the effect of several elements was investigated. Results are shown in Figure 5, where the phase stability as a function of Al, C, Cr, Co, Nb, Ta and Ti is plotted. In all of these cases, the base composition was that of IN939 (Table 1) and one element was varied at a time. The results reveal the complex interactions that take place to determine the phase stability at any given temperature. Figure 5 shows that increasing levels of Al, Cr, Co, Nb, Ta, and Ti all lead to higher sigma phase contents, while increasing C leads to a decrease in sigma phase. The effects of Cr and Co are straightforward,

since these are the primary elements in sigma phase, and higher levels can be expected to lead to higher levels of sigma phase. The effect of Cr is noticeably stronger than that of Co. The beneficial influence of C in reducing sigma phase is due to the fact that higher C leads to more carbide formation, and in particular more $M_{23}C_6$, which is very rich in Cr. Thus, higher C levels take up Cr, leaving less Cr that is available to form sigma phase. Similar kinds of interactions prevail for Nb and Ta additions. As Nb and Ta levels increase, the stability of $M_{23}C_6$ is reduced in favor of MC. Since MC is not rich in Cr but $M_{23}C_6$ is very rich in Cr, stabilizing MC at the expense of $M_{23}C_6$ frees up Cr and it is then available to form sigma phase. The influence of Al and Ti is yet another example of complex phase interactions. As Al and Ti are increased, gamma prime is stabilized and the balance between gamma and gamma prime is shifted toward more gamma prime. Since Cr partitions to gamma phase, and not to gamma prime, the formation of more gamma prime leads to more Cr in the remaining matrix, and higher levels of Cr lead, in turn, to higher sigma phase quantities. Thus, the calculations can be used to identify the influence of individual constituents on phase stability. Furthermore, the calculations show quite complex behavior that may not be apparent at first, but are readily explained upon closer examination.

It is important to examine the evolution of carbides and their compositions as a function of temperature in these alloys. This is shown in Figures 6 and 7 for the nominal IN738 composition in Table 1. Figure 6 is a higher magnification view of Figure 1a, showing the phase fractions (wt %) as a function of temperature for the minor constituents. This plot clearly shows that MC carbide is stable at high temperatures, but at lower temperatures it becomes unstable and is replaced by $M_{23}C_6$. Figure 7 shows the composition of these two carbides as a function of temperature. The MC carbide is primarily a titanium carbide, and is stable at very high temperatures. As the temperature drops, the calculations show that the equilibrium composition of the MC carbide changes, as some titanium is replaced by niobium and tantalum. This is related to the concurrent increase in the gamma prime fraction (see Figure 1a), and the fact that titanium partitions to the gamma prime. The $M_{23}C_6$ carbide is Cr rich and its composition remains quite stable over the entire temperature range where it is found. The composition evolution of the MC carbide and its replacement by $M_{23}C_6$ at lower temperatures has important consequences. The change in MC composition can take place by two possible mechanisms: there could be a gradual, diffusion-controlled replacement of Ti by Nb or Ta in existing carbides, or new MC carbides could form as previously existing TiC dissolves. Which mechanism will take place will have a strong impact on the microstructure. If the TiC gradually shifts in composition, the distribution of carbides will remain the same. Since these carbides form in the liquid (see Figure 1a), they are likely to be uniformly distributed throughout the microstructure. However, if new MC carbides form as TiC carbides dissolve, they may be located at preferential sites such as grain boundaries. The substitution of MC carbide by $M_{23}C_6$ carbides at lower temperatures will also have an impact on the microstructure. Once again, $M_{23}C_6$ carbides are likely to preferentially nucleate along grain boundaries and this inhomogeneous distribution will replace the uniformly distributed MC carbides that formed directly from the liquid. Finally, the evolution of the carbides indicates that the specific carbides that will be present will depend to a large extent upon the heat treatments; sufficient exposure at high temperatures will be necessary

in order for the TiC carbides to be replaced by more Nb- and Ta-rich MC carbides or to $M_{23}C_6$ carbides.

The evolution of carbides is more dramatic if one considers an addition of 0.5 Hf to the IN738 composition in Table 1. The composition of the MC carbides in such a Hf-modified alloy is shown in Figure 8a. At ~ 1000°C, the equilibrium MC carbide composition changes dramatically, from a Ti-Nb-Ta-rich carbide to a Hf-rich carbide (kinetics will determine to what extent this change actually takes place). The composition change is over the same general temperature range where the MC carbides become less stable with respect to $M_{23}C_6$ carbide. The calculations also show that significant changes in the carbide stability can be expected with small additions of Hf as well. With 0.5 wt % Hf, the MC carbide stability range is extended to lower temperatures, and overlaps much more with the stability range of $M_{23}C_6$, as shown in Figure 8b (compare with Figure 6, same alloy without Hf). These calculations also indicate that correspondingly important changes in the microstructure may follow. These types of calculations reveal potential changes that may have a strong impact on the mechanical properties as well.

Additional Considerations

The results that have been presented show a wide range of behavior with respect to phase stability and associated microstructure development that can be predicted with the use of computational thermodynamics. However, several additional features must be taken into consideration when attempting to develop new, improved, and optimized alloys based on such calculations. First, the calculations represent equilibrium results. This has several consequences. When dealing with welding issues, segregation during solidification can lead to many non-equilibrium effects. Some phases that are not stable in equilibrium may become stable as a result of solute enrichment during solidification. These effects can be simulated to some degree by performing Scheil solidification calculations using the same computational thermodynamic software. Such calculations will provide insight as to what deviations from equilibrium might be expected. Second, the calculations also do not consider phase transformation kinetics. Therefore, while sigma phase may be predicted over a given temperature range, sigma phase formation may be very sluggish and it may never be observed under many conditions. Once again, the effects of sluggish kinetics can be taken into account in the calculations by simply removing a slow-forming phase from consideration when determining the mix of phases that are present at any given temperature. Such calculations can be used to identify short-term phase stability versus long-term phase stability. Finally, the continuous variation in phase stability and phase composition as a function of temperature will require extensive diffusion before the equilibrium microstructure is attained. Thus, for example, heat treatments at several different temperatures may result in the formation of different carbides and these may remain present in the microstructure for extended times before the unstable phases finally yield to the equilibrium phases. Therefore, one must allow for such kinetic considerations when trying to predict the microstructure after any given heat treatment or service-exposure. Some kinetics calculations based on a diffusion-controlled mechanism tied in

with the computational thermodynamics approach are possible with available software (1). Other packages using an empirical approach to assess limited kinetics effects are also available (5).

The computational thermodynamics calculations can also be used to identify potential optimum heat treatment schedules. For example in Figure 1, the solution temperature range in which gamma prime is not stable can be readily identified. Furthermore, sequential heat treatments can be determined. Referring to Figure 1c, if a solution heat treatment at 1200°C, producing a nearly 100% gamma microstructure (with a small amount of MC carbide) is followed by a heat treatment at 1050°C, then precipitation of roughly 25% gamma prime can be expected. This is only half of the final, low temperature amount of gamma prime that is expected; the gamma prime content appears to level off at approximately 52 wt %. Thus, if the alloy is cooled quickly to room temperature from 1050°C, it is likely that significant secondary gamma prime will form during cooling. On the other hand, if the alloy is slowly cooled from 1050°C, or if it is cooled to, say 950°C and held there before cooling to room temperature, then one can expect that the existing gamma prime will grow at the expense of the gamma matrix, rather than nucleating secondary gamma prime, and the result will be a coarser but more uniform distribution of gamma prime in the gamma matrix. Therefore, computational thermodynamics can provide valuable information on heat treatment schedules and the phase transformations that can be expected as a result of heat treating.

Finally, some remarks regarding the accuracy of the computational thermodynamics calculations are necessary. The calculations are completely dependent upon the accuracy of the parameters in the various databases. Specialty databases have been developed for nickel-based superalloys. In the development process, the parameters in the free energy functions are based on experimental results, and therefore they should be reasonably reliable. Calculations for alloy compositions that do not represent extreme deviations from the commercial alloys that were used to generate the data should be accurate. The benefit of using the computational thermodynamics approach is that the intricate and complex interactions in multi-component systems (alloys in this study contained up to 12 components) are modeled. Even in cases where large extrapolations from conventional alloy compositions are made, the computational thermodynamics approach may be far more accurate than approximate conclusions drawn from simple binary and ternary phase diagrams (if they are even available).

Summary and Conclusions

Computational thermodynamics was used to investigate the influence of modifications to the compositions of gamma-prime-strengthened nickel-based superalloys in an effort to improve potential weldability and performance of welded materials. The calculations were made for multi-component alloy compositions, and they showed that this approach is capable of identifying the complex interactions among alloying additions. The stability of carbides and the transformation from elevated MC carbides to low temperature $M_{23}C_6$ carbides was shown to be very sensitive to composition. It was demonstrated how computational thermodynamics could

be used to identify the compositional requirements to avoid the formation of deleterious phases such as eta phase, sigma phase and P-phase. In addition, it was shown how the calculations can provide valuable information with regard to identifying optimum heat treatment schedules. These results indicate that the alloy development process can be streamlined substantially with the use of modeling tools.

Acknowledgments

This research was performed at the Oak Ridge National Laboratory and sponsored by the Electric Power Research Institute, Inc. under the Work-for-Others Program, IAN # 14B507801, with the U.S. Department of Energy under contract DE-AC05-00OR22725 with UT-Battelle, LLC. The authors would also like to thank W. F. Hehmann and Y. Hu of Honeywell Aerospace Services for many stimulating and fruitful discussions and for preparing and evaluating many of the trial alloys and welds.

References

1. J-O. Andersson, T. Helander, L. Höglund. P. Shi and B. Sundman, "THERMOCALC and DICTRA, Computational Tools for Materials Science," *Calphad* 2002, 26(2), 273-312.

2. R. H. Davies, A. T. Dinsdale, J. A. Gisby, J. A. J. Robinson and S. M. Martin, "MTDATA – Thermodynamic and Phase Equilibrium Software from the National Physical Laboratory," *Calphad* 2002, 26(2), 229-271.

3. C. W. Bale, P. Chartrand, S. A. Degterov, G. Eriksson, K. Hack, R. Ben Mahfoud, J. Melançon, A. D.Pelton and S. Petersen, "FactSage Thermochemical Software and Databases, *Calphad* 2002, 26(2), 189-228.

4. S.-L. Chen, S. Daniel, F. Zhang, Y. A. Chang, X.-Y. Yan, F.-Y. Xie, R. Schmid-Fetzer and W. A. Oates, "The PANDAT Software Package and its Applications," *Calphad* 2002, 26(2), 175-188.

5. N. Saunders, X. Li, A. P. Miodownik and J-Ph. Schille, "Computer Modelling of Materials Properties," p 185-197 in *Materials Design Approaches and Experiences*, eds. J.-C. Zhao, M. Fahrmann and T. Pollock, TMS, Warrendale, PA, 2001.

6. Ni-DATA version 5, ThermoTech Ltd. Surrey Technology Centre, Guildford, England

Table 1: Typical Alloy Compositions Used in the Calculations (wt %)

Element	IN738	IN939	Rene80	GTD111	IN625
Al	3.4	1.9	3.0	3.0	0.4
B	0.01	0.01	0.015	0.01	-
C	0.10	0.15	0.17	0.10	0.1
Co	8.5	19.0	9.5	9.5	1
Cr	16.0	22.5	14.0	14.0	22
Fe	-	-	-	-	5
Mo	1.75	-	4.0	1.5	9
Nb	0.9	1.0	-	-	3.6
Ta	1.75	1.4	-	2.8	-
Ti	3.4	3.7	5.0	4.9	0.4
W	2.6	2.0	4.0	3.8	-
Zr	0.05	0.1	0.03	0.03	-
Ni	balance	balance	balance	balance	balance

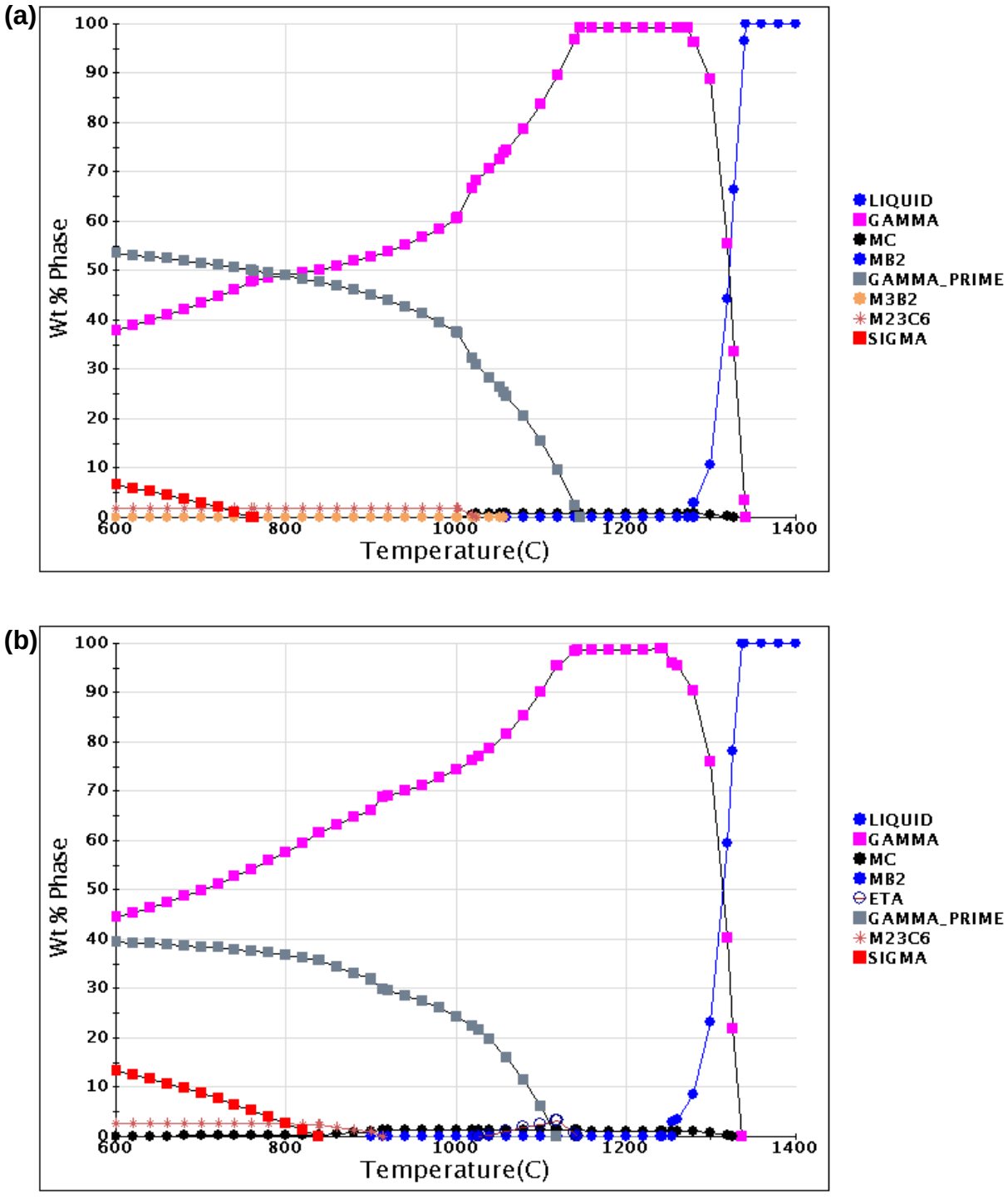

Figure 1: Calculated distribution of phases (wt %) versus temperature for (a) IN738, (b) IN939, (c) Rene80 and (d) GTD111 (see Table 1 for compositions).

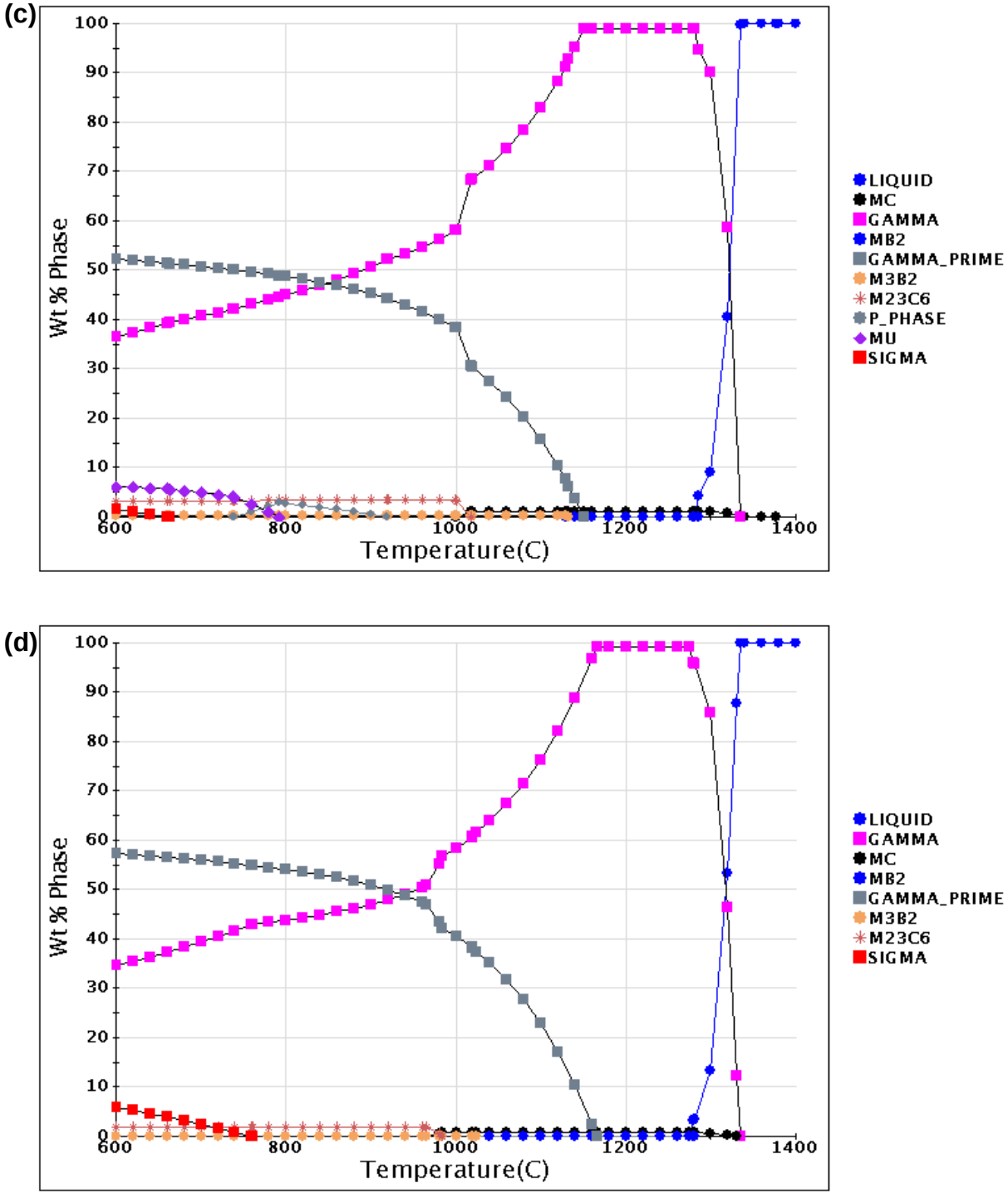

Figure 1 (cont'd): Calculated distribution of phases (wt %) versus temperature for (a) IN738, (b) IN939, (c) Rene80 and (d) GTD111 (see Table 1 for compositions).

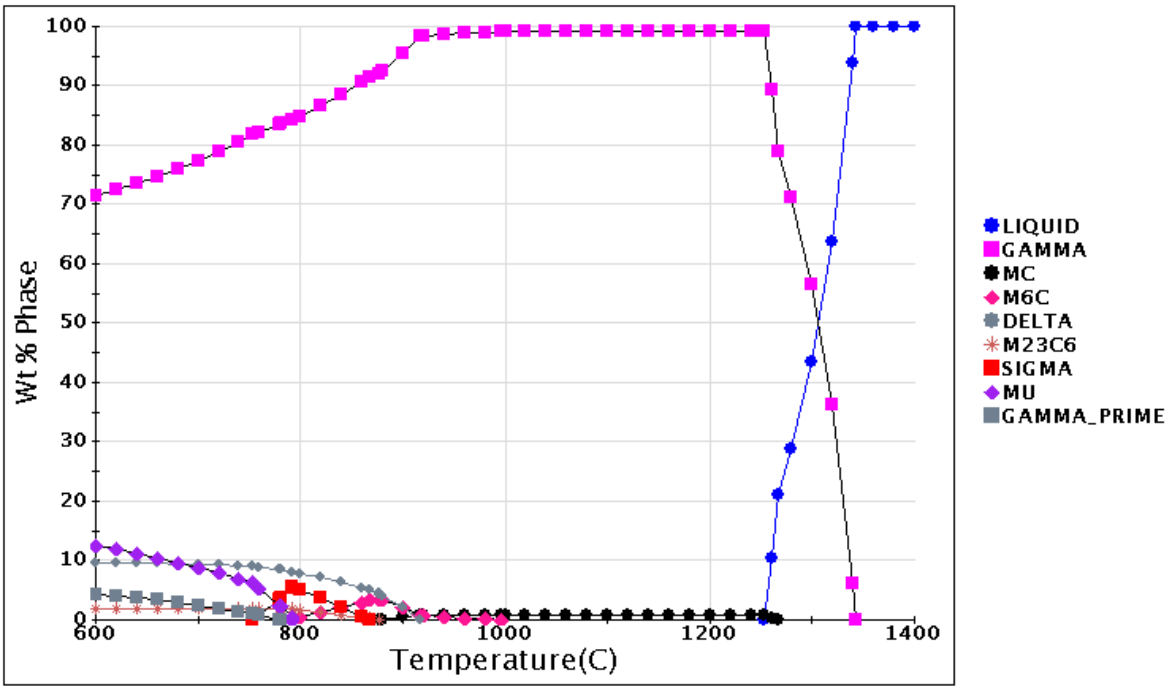

Figure 2: Calculated distribution of phases (wt %) versus temperature for IN625 (see Table 1 for compositions).

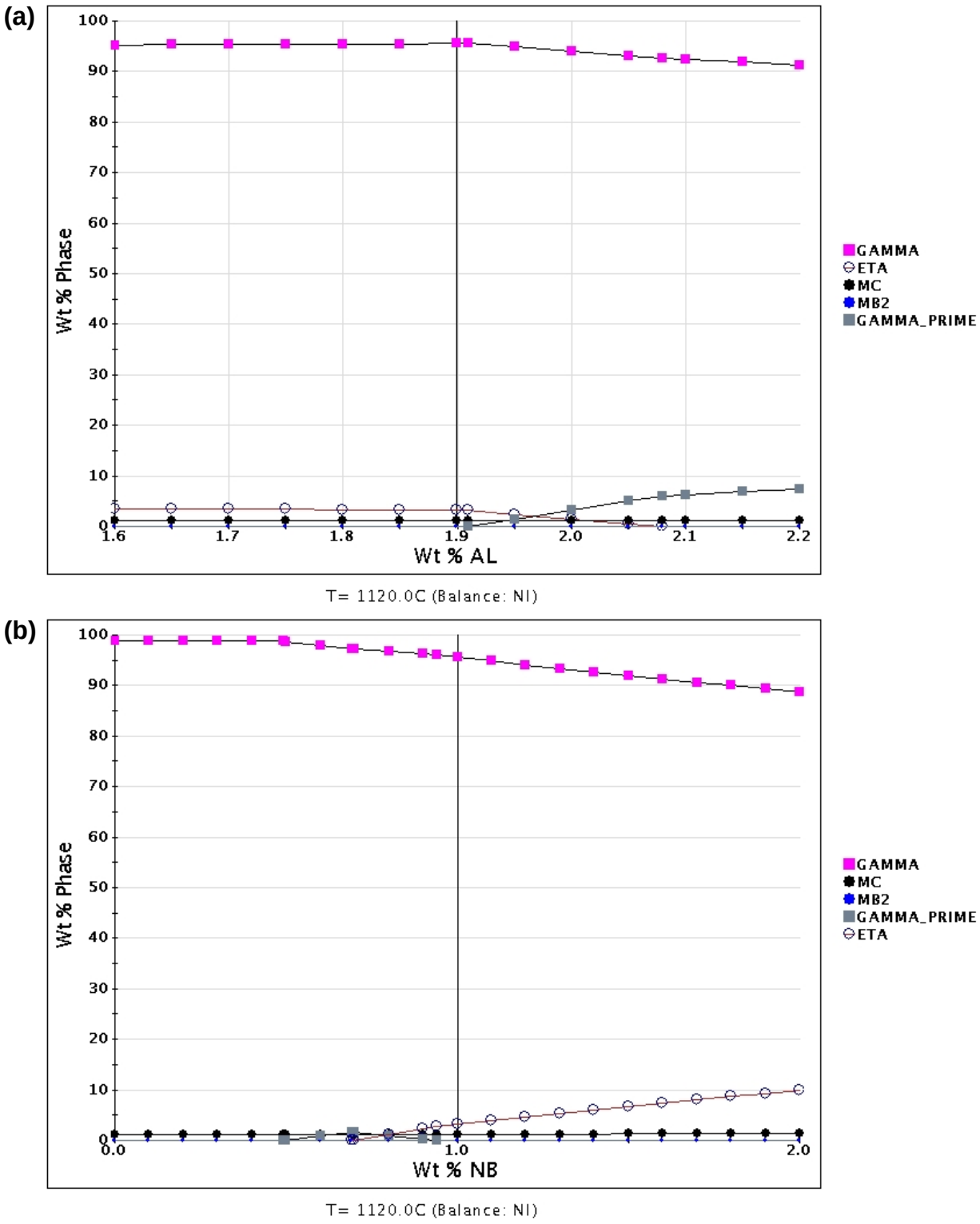

Figure 3: Phase stability in IN939 at 1120°C as a function of (a) Al and (b) Nb, holding all other elements constant (see Table 1 for values).

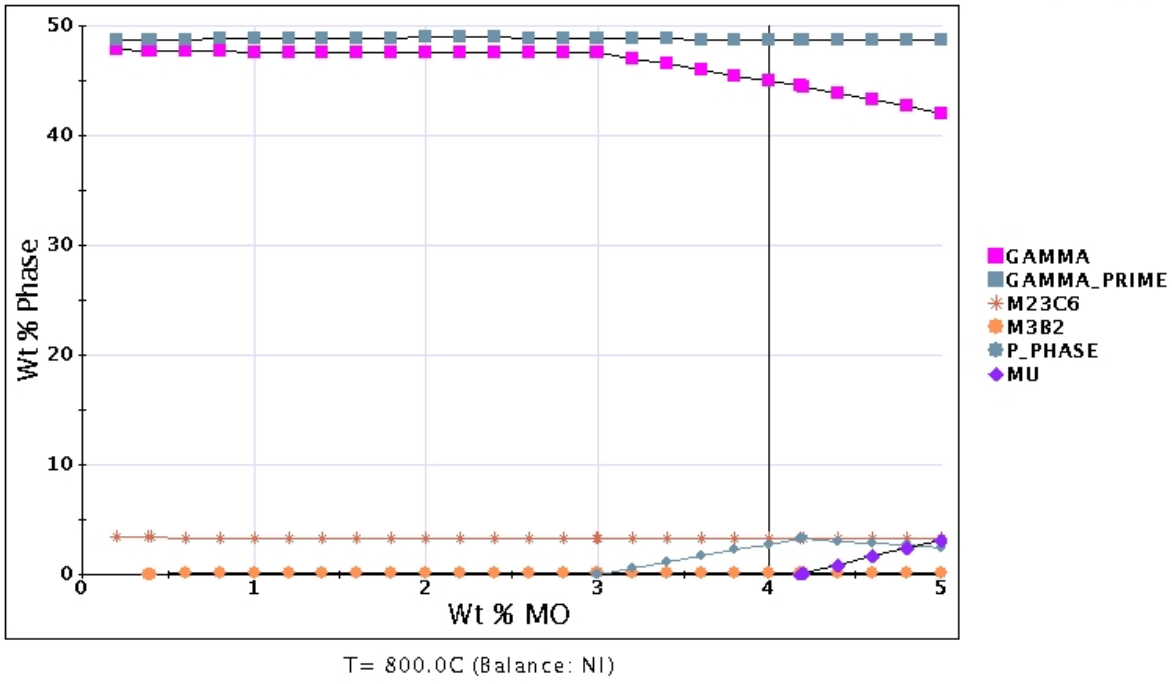

Figure 4: Phase stability in Rene80 at 800°C as a function of Mo, holding all other elements constant (see Table 1 for values).

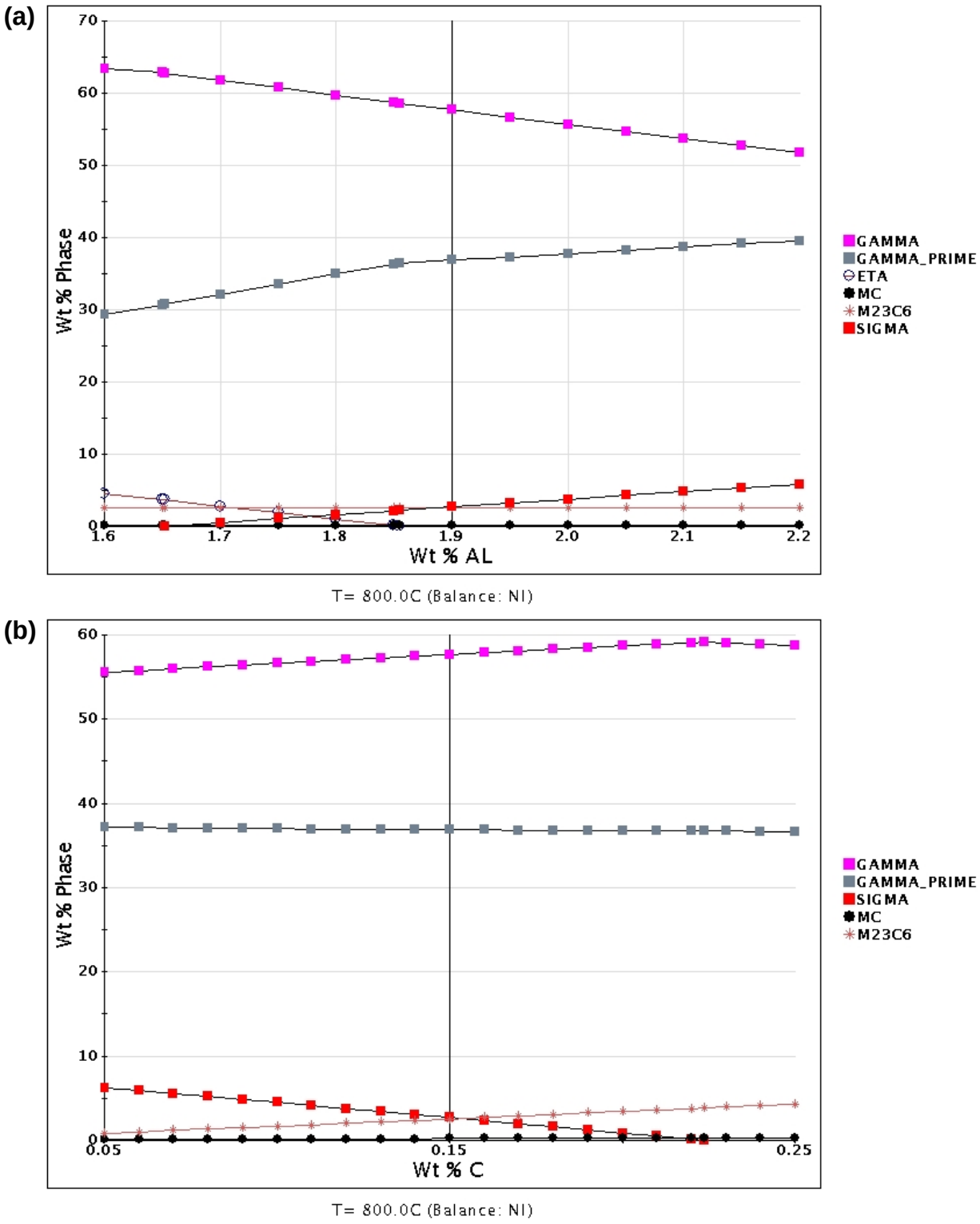

Figure 5: Phase stability in alloy IN939 at 800°C as a function of (a) Al , (b) C, (c) Cr, (d) Co, (e) Nb, (f) Ta, and (g) Ti (varying only one element at a time).

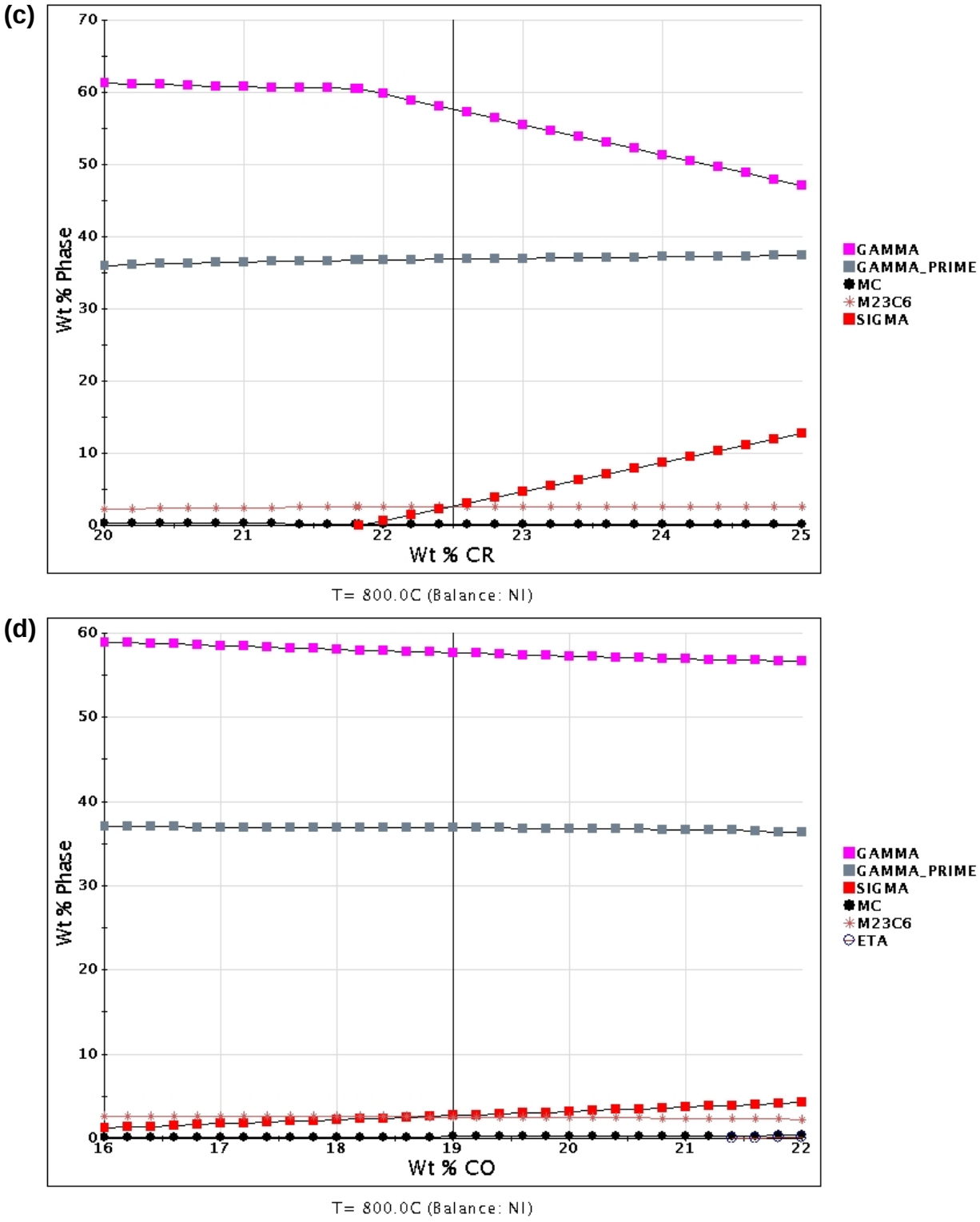

Figure 5 (cont'd): Phase stability in alloy IN939 at 800°C as a function of (a) Al , (b) C, (c) Cr, (d) Co, (e) Nb, (f) Ta, and (g) Ti (varying only one element at a time).

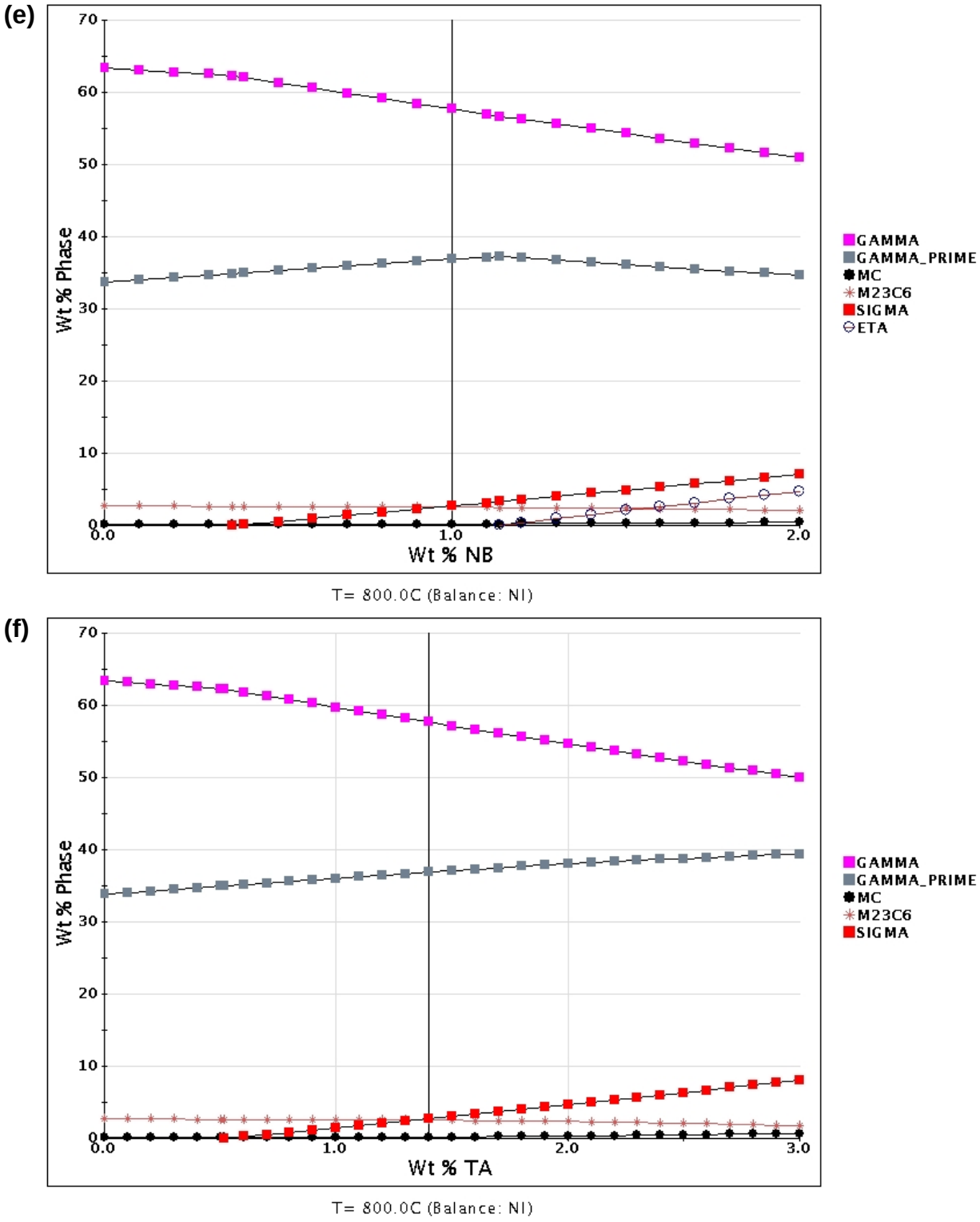

Figure 5 (cont'd): Phase stability in alloy IN939 at 800°C as a function of (a) Al , (b) C, (c) Cr, (d) Co, (e) Nb, (f) Ta, and (g) Ti (varying only one element at a time).

(g)

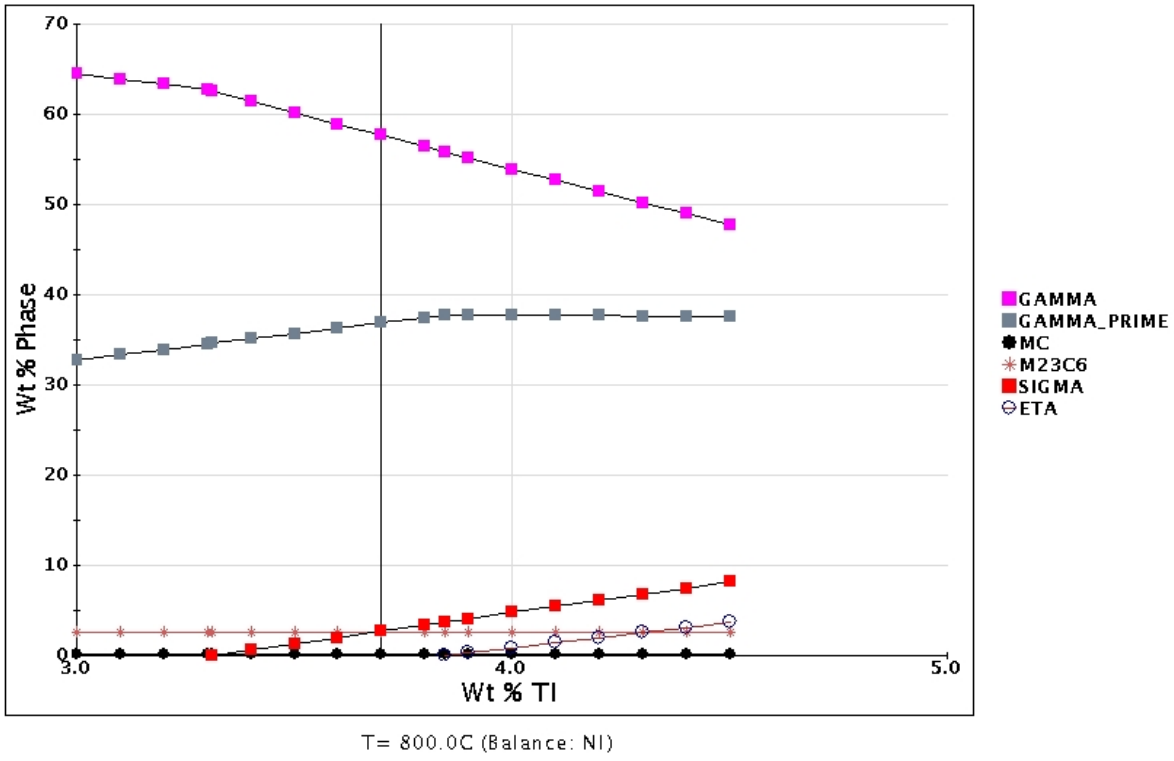

Figure 5 (cont'd): Phase stability in alloy IN939 at 800°C as a function of (a) Al , (b) C, (c) Cr, (d) Co, (e) Nb, (f) Ta, and (g) Ti (varying only one element at a time).

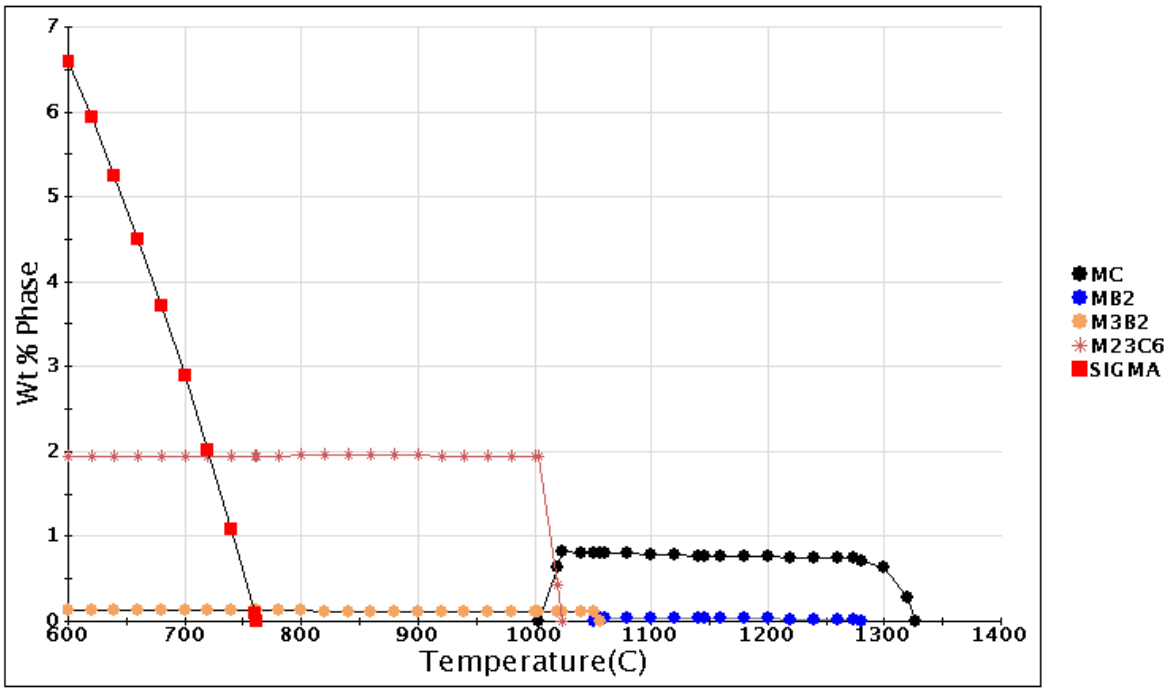

Figure 6: Detailed view of minor phase constituents versus temperature in IN738

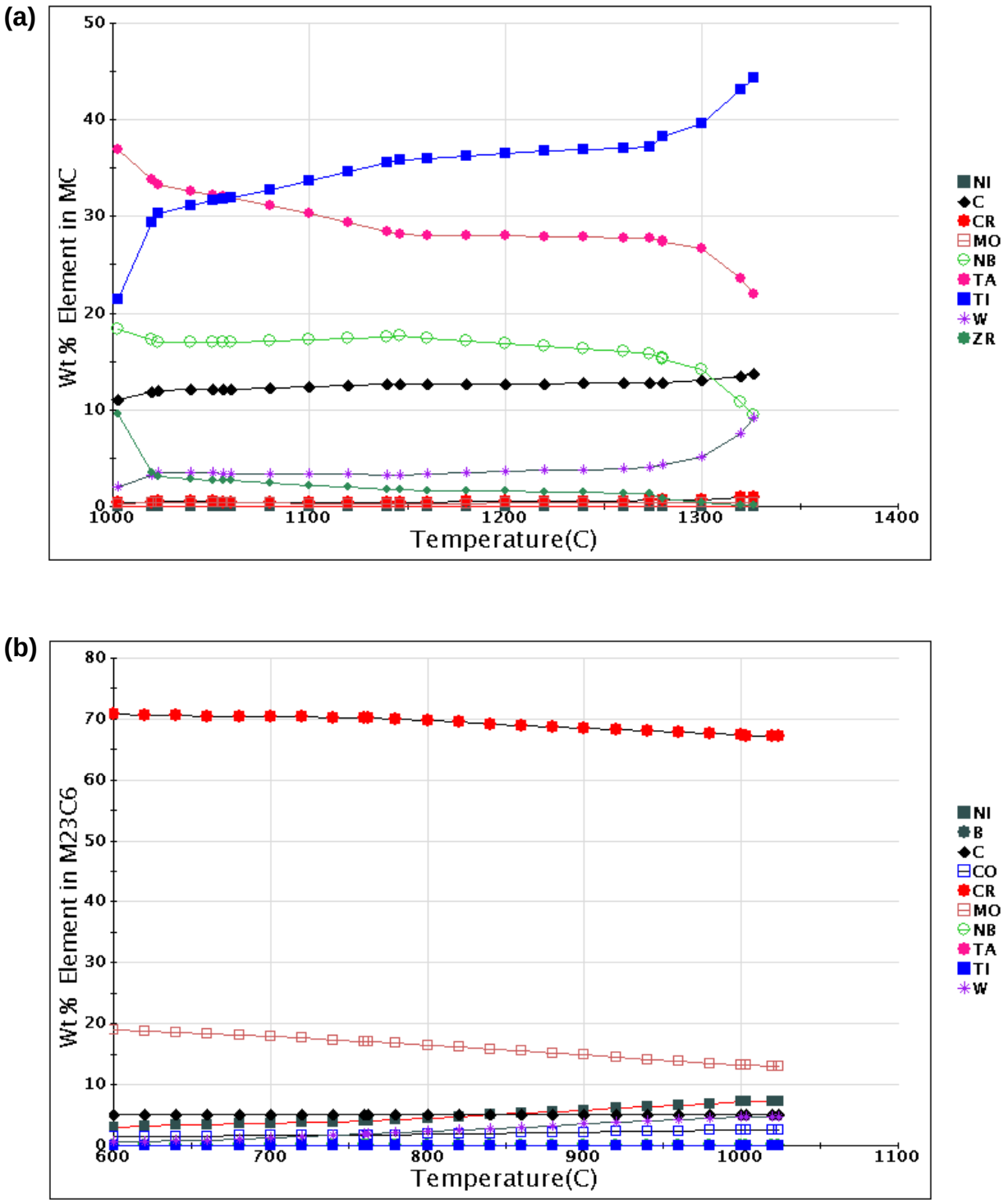

Figure 7: Equilibrium composition of (a) MC carbide and (b) $M_{23}C_6$ carbide in IN738 as a function of temperature.

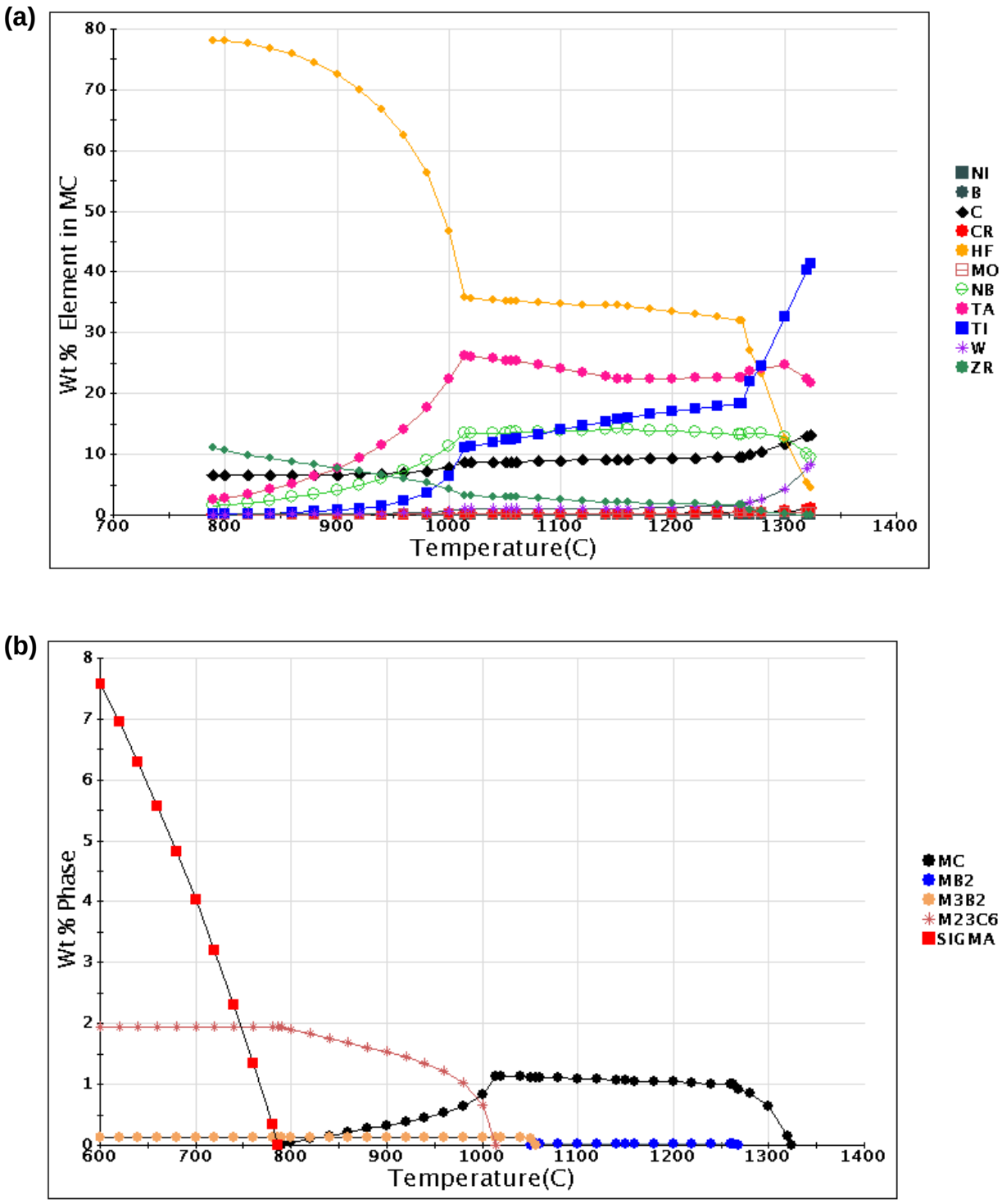

Figure 8: Calculations for IN738 modified with an addition of 0.5 wt % Hf. (a) composition of MC carbide versus temperature and (b) phase distribution of minor phases versus temperature.